

Ventral aspect of the visual form pathway is not critical for the perception of biological motion

Sharon Gilaie-Dotan^{a,b,1}, Ayse Pinar Saygin^c, Lauren J. Lorenzi^d, Geraint Rees^{a,b}, and Marlene Behrmann^{d,e}

^aInstitute of Cognitive Neuroscience and ^bWellcome Trust Centre for Neuroimaging, Institute of Neurology, University College London, London, WC1N 3AR, United Kingdom; ^cDepartment of Cognitive Science and Neurosciences Program, University of California, San Diego, CA 92093-0515; and ^dDepartment of Psychology and ^eCenter for the Neural Basis of Cognition, Carnegie Mellon University, Pittsburgh, PA 15213

Edited by Michael E. Goldberg, Columbia University College of Physicians and Surgeons and the New York State Psychiatric Institute, New York, NY, and approved December 12, 2014 (received for review August 6, 2014)

Identifying the movements of those around us is fundamental for many daily activities, such as recognizing actions, detecting predators, and interacting with others socially. A key question concerns the neurobiological substrates underlying biological motion perception. Although the ventral “form” visual cortex is standardly activated by biologically moving stimuli, whether these activations are functionally critical for biological motion perception or are epiphenomenal remains unknown. To address this question, we examined whether focal damage to regions of the ventral visual cortex, resulting in significant deficits in form perception, adversely affects biological motion perception. Six patients with damage to the ventral cortex were tested with sensitive point-light display paradigms. All patients were able to recognize unmasked point-light displays and their perceptual thresholds were not significantly different from those of three different control groups, one of which comprised brain-damaged patients with spared ventral cortex ($n > 50$). Importantly, these six patients performed significantly better than patients with damage to regions critical for biological motion perception. To assess the necessary contribution of different regions in the ventral pathway to biological motion perception, we complement the behavioral findings with a fine-grained comparison between the lesion location and extent, and the cortical regions standardly implicated in biological motion processing. This analysis revealed that the ventral aspects of the form pathway (e.g., fusiform regions, ventral extrastriate body area) are not critical for biological motion perception. We hypothesize that the role of these ventral regions is to provide enhanced multiview/posture representations of the moving person rather than to represent biological motion perception per se.

ventral stream | visual form agnosia | action perception | EBA | point-light displays

Perception of the movements of other peoples’ bodies is fundamental to our daily interactions (e.g., motor learning, social interactions, anticipating actions of others), and is sufficiently robust so as to succeed even under suboptimal conditions [e.g., poor illumination and even partial occlusion (1–6)]. A clear demonstration of the resilience of this ability is the ease with which people recognize biological motion from point-light displays (PLDs) that consist of only a small set of moving points that mark joints on the body (7), (Fig. 1A, *Left*). These stimuli appear to naive observers as a set of incoherent dots when static, but evoke a vivid percept of a moving person when in motion. Observers are able to infer movement information, such as the motion or direction of the figure, in these impoverished PLDs even under conditions of masking, added noise (8–11), or night driving (3, 4, 12).

Examination of the neural correlates of the perception of body movement reveals a widespread cortical network (13). Because biological motion perception, in natural vision or in PLDs, involves both form and motion perception (14), unsurprisingly, cortical regions associated with both form and motion perception are activated. It is unclear, however, whether all of these brain areas contribute causally to the perception of biological motion. Neuropsychological studies in patients and transcranial magnetic stimulation (TMS) studies in normal observers have identified

several motion-sensitive areas as critical for biological motion perception, including the posterior superior temporal sulcus (pSTS) and ventral premotor cortex (vPMC) (11, 15–17), given that a sustained or transient lesion to these regions impairs biological motion perception. However, whether form-sensitive regions in the ventral “form” visual pathway [for example, the extrastriate body area (EBA) (18–20) in the lateral occipital cortex], which are consistently activated in response to biological motion in neuroimaging studies, play a critical role in biological motion perception remains unknown.

PLDs constitute ideal stimuli with which to explore whether the engagement of the ventral visual cortex is necessary for biological motion perception, as these displays permit the presentation of recognizable body movements while dissociating them from “classic ventral” form cues, such as contour, surface, shape, texture, and color. As such, PLDs are thought to depict dynamic body and action information solely via motion cues. To the extent that the ventral form pathway is involved in PLD perception, this cannot be attributed to processing classic ventral form cues. Even in the absence of classic form cues, however, moving PLDs convey coarse form information of the dynamic body, and investigating the structure of the articulated body that can be retrieved from the coherent movement of the dots has been a central driving motivation in biological motion research (e.g., refs. 21–27). This approach has been true since the pioneering work of Johansson (7), and therefore, unsurprisingly, these displays have often been termed biological structure-from-motion or form-from-motion. In light of the above, whether the processes supporting biological motion perception—in the absence of classic form cues—critically

Significance

Perceiving the movements of people around us is critical for many daily skills (from detecting threats to social interactions) and involves both form and motion perception. Even though the “form” visual pathway is standardly activated by biological motion stimuli, it is unknown whether this pathway’s integrity is critical for the perception of biological motion. Here, we examined whether damage to different aspects of the form pathway affects biological motion perception. Individuals with lesions to the ventral aspects of this pathway evinced normal biological motion perception despite their impairments in form perception. Our counterintuitive findings indicate that biological motion can be perceived and processed normally even when the ability to perceive the form or the actor executing the movements is impaired.

Author contributions: S.G.-D., A.P.S., G.R., and M.B. designed research; S.G.-D., A.P.S., and L.J.L. performed research; A.P.S. contributed new reagents/analytic tools; S.G.-D. and A.P.S. analyzed data; and S.G.-D., A.P.S., G.R., and M.B. wrote the paper.

The authors declare no conflict of interest.

This article is a PNAS Direct Submission.

Freely available online through the PNAS open access option.

¹To whom correspondence should be addressed. Email: shagido@gmail.com.

This article contains supporting information online at www.pnas.org/lookup/suppl/doi:10.1073/pnas.1414974112/-DCSupplemental.

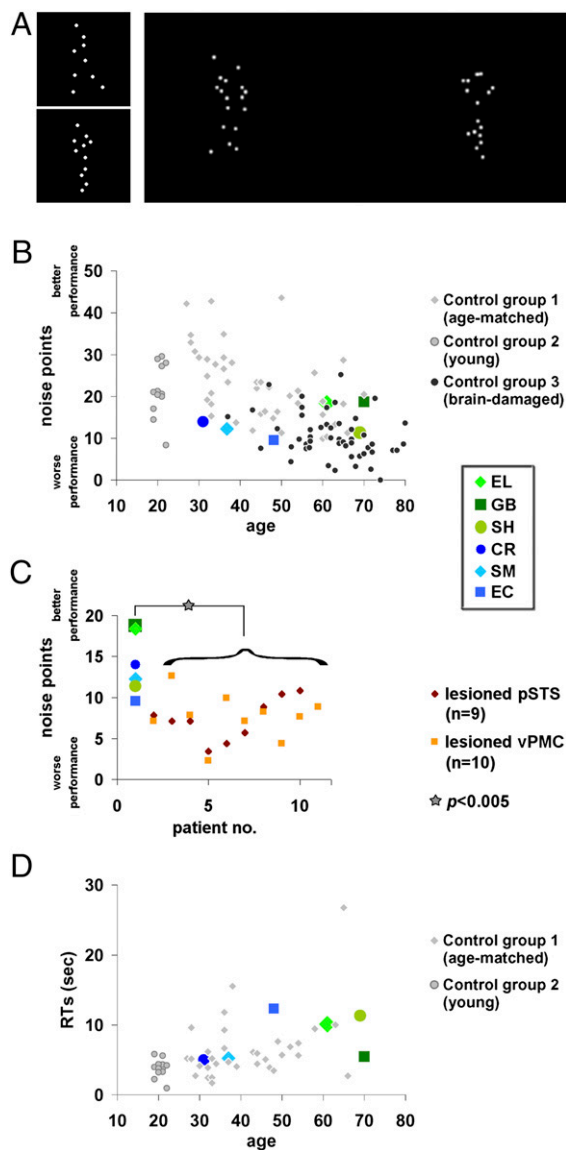


Fig. 1. Biological motion perception: Exp. 1 paradigm and results. (A, *Left*) Static snapshots from the unmasked PLDs presented in the action recognition phase; participants were required to verbally describe the display. (*Right*) To determine perceptual thresholds, two masked PLDs embedded in noise points were presented simultaneously, one on the right and one on the left, one containing a biological movement (here on the left), and the other a spatially scrambled version of that movement. The task was to determine which side contained the moving human figure. The noise points were added adaptively according to individual performance (*Methods*). (B) Individual perceptual thresholds (*y* axis) of the ventral visual patients and the three control groups against age (*x* axis). Perceptual thresholds represent the number of noise points that can be tolerated while performing at 82% accuracy (more noise points correspond to better performance). Each ventral patient was not significantly different from any of the control groups, and performed similarly to or better than the brain-damaged controls with spared ventral cortex (11) (Table 2). (C) Ventral visual patients' performance was significantly better than that of brain-damaged controls (11) whose lesions invaded regions critical for biological motion perception (pSTS, vPMC). (D) Response times (*y* axis) as recorded during the experiment plotted against age (*x* axis). Response times are not very informative as instructions did not require speeded responses (participants were able to respond leisurely and take breaks). Response times of the brain-damaged control group were not available. Ventral visual patients' response times (apart from EC) (*Results*) were not significantly slower than those of their age-matched controls.

depend on the form computations of the form visual pathway still remains unknown (20, 28–30).

One way to address this issue is to study whether damage to the ventral “form” visual pathway affects the perception of biological motion. The predictions are straightforward: if ventral stream integrity and ventral form representations are necessary for the perception of biological motion, then individuals with form perception deficits following damage to the ventral visual cortex [including damage to specific areas implicated in biological motion processing or areas implicated in body form perception (e.g., the EBA) (18–20)], should be impaired at perceiving biological motion.

To examine this hypothesis, we tested a group of six patients with form perception deficits following a circumscribed lesion to the ventral visual cortex in adulthood (Table 1). Using PLDs and paradigms that are successful in detecting biological motion perceptual deficits following brain damage (11, 17), we measured the patients' recognition and perception of biological motion in two different experiments. We compared each patient's performance to that of three different control groups: (i) a brain-damaged control group of 54 patients, whose cortical lesions fell outside of the ventral visual cortex; (ii) a group of healthy age-matched controls (patient-specific); and (iii) a group of 13 young control participants. The importance of the brain-damaged control group is twofold. First, comparing the ventral patients to patients with nonventral lesions allowed us to determine whether biological motion perception, if affected, is specifically a consequence of a ventral lesion or of brain damage, more generally. Second, because a subset of patients in the nonventral control group have lesions to brain areas known to significantly impair biological motion perception (pSTS and vPMC), we were able to compare directly the perceptual thresholds of the ventral patients with those of individuals with identified deficits in biological motion following damage to the pSTS or vPMC. Finally, given that the ventral cortex constitutes a large swath of the cortex and that patients' lesions were not identical, we assessed the brain–behavior correspondences further by examining, at a finer grain, which—if any—affected subareas impair biological motion perception. To do so, for each patient we carefully delineated the lesion, assessed the magnitude of the damage, and situated the lesion relative to regions in the ventral, lateral, and middle temporal cortex that are standardly associated with biological motion processing, including body parts and visual motion-sensitive regions (e.g., refs. 13, 14, 20, 31–33).

To anticipate our findings, we show that biological motion recognition and perceptual thresholds of the ventral patients consistently fall within the normal range of all three control groups. Thus, our results indicate that the perception of biological motion (i) does not depend on the integrity of the ventral aspects of the form visual pathway or on the integrity of the ventral portion of the EBA (ventral to the human middle temporal V5 complex, MT+/V5), and (ii) can be dissociated from form perception. We conclude, therefore, that computations that suffice for the perception of biological motion are mediated by mechanisms independent of the form ventral cortex, and that such computations may be based on motion cues that represent movement kinematics rather than on form information per se.

Results

Experiment 1. Recognition and perceptual thresholds for biological motion.

At the start of Exp. 1, participants were presented with unmasked PLDs (Fig. 1A, *Left*) and were asked to describe what they perceived. For these unmasked PLDs, all six ventral patients (as well as almost all individuals in three groups of controls) were able to name the movements effortlessly and immediately, even without prior knowledge of or training on PLDs. This observation is consistent with previous work showing that patients are generally able to recognize unmasked PLDs of biological motion (34–39). Only two of the control patients with brain-damage outside of the

Table 1. Summary of the visual perceptual functions and impairments of the six ventral patients

Function/Impairment	EL	GB	SH	CR	SM	EC
Lesioned hemisphere	Left	Left	Left	Right (+ left)	Right	Right
Age (sex)	61 (F)	70 (F)	69 (M)	31 (M)	37 (M)	48 (F)
Time from injury	15 y	3 y	6 y	15 y	19 y	8 y
Visual acuity	Corrected to normal	Corrected to normal	Corrected to normal	Normal	Normal	Normal
Accommodation/convergence deficit	None apparent or reported	None apparent or reported	None apparent or reported	None apparent or reported	None apparent or reported	None apparent or reported
Visual field	Upper right quadrantanopia	Upper right quadrantanopia	Right homonymous hemianopia (largely resolved)	Full field	Full field	Full field
Object perception	Mild impairment (1–2 SDs)	Mild impairment (1–2 SDs)	Mild impairment (1–2 SDs)	Agnosic (3 SDs)	Agnosic (3 SDs)	Object recognition difficulties (screening)
Face perception	Mild impairment (1–2 SDs)	Mild impairment (1–2 SDs)	Mild impairment (1–2 SDs)	Prosopagnosic (3 SDs)	Prosopagnosic (3 SDs)	Face recognition difficulties (screening)
Word perception	Pure alexic (3 SDs)	Pure alexic (3 SDs)	Pure alexic (3 SDs)	Mild impairment (1–2 SDs)	Mild impairment (1–2 SDs)	Unknown
Motion perception – basic (detection)	Normal	Normal	Unknown	Impaired (very slow motion)	Impaired (very slow motion)	Impaired (very slow motion)
Motion perception – basic (coherence)	Normal	Normal	Unknown	Impaired (very fast motion)	Impaired (medium to very fast motion)	Unknown
Motion perception – structure (SFM)	Normal	Normal	Unknown	Impaired	Impaired	Impaired
Motion perception – biological unmasked PLDs (Exp. 1)	Normal	Normal	Normal	Normal	Normal	Normal
Motion perception – biological perceptual thresholds (Exp. 1)	Normal	Normal	Normal	Normal	Normal	Normal
Motion perception – biological unmasked PLDs (Exp. 2)	Normal	Normal	Normal	Normal	Normal	Normal
Motion perception – biological perceptual thresholds (Exp. 2)	Normal	Normal	Normal	Normal	Normal	Normal

Most of these data have been reported earlier [EL (61, 70–75), GB (61, 75), SH (70, 75), CR (61, 65–67, 70), SM (61, 64–69), EC (61)]. The data from this study are presented in the four bottom rows. We summarize the patients' abilities by noting the number of SDs each score deviates from the controls' mean. Visual impairments are denoted in bold.

ventral cortex (from the “brain-damaged control group” in the present study) were unable to recognize unmasked PLDs (11).

After this recognition phase, perceptual thresholds for biological motion (number of noise points at which performance is 82% accurate; see Fig. 1A, Right, for illustration) were measured for all participants (Fig. 1B, and detailed in Table 2). Consistent with previous results showing that the perceptual thresholds of brain-damaged patients for biological motion are significantly lower than those of healthy age-matched controls (11), four of the ventral visual patients' (CR, SM, EC, and SH) perceptual thresholds were at the lower end of their matched controls' distribution (control group 1; light diamonds in Fig. 1B), but not statistically different (see Table 2 for statistical details). Moreover, the perceptual threshold of each ventral patient was also

within the norm of the younger control group [control group 2; all $|t_{(12)}|s < 1.44$, all P s > 0.17 (40); Fig. 1B, light gray circles].

We then compared the thresholds of the ventral patients and those of 54 patients with unilateral nonventral brain damage [control group 3 (11); dark circles in Fig. 1B]. If the integrity of the ventral visual cortex is critical for biological motion perception, then the performance of the ventral visual patients should be significantly poorer than that of patients with brain damage elsewhere. In contrast, the ventral patients' thresholds were trending to be significantly better than their brain-damaged controls [Wilcoxon nonparametric rank-sum test: ventral patients (median = 13.11, $n = 6$) vs. brain damaged controls (median = 9.82, $n = 54$): $U = 258$, $P = 0.06$]. In addition, in an individual case analysis, each of the ventral visual patients' performance was better than the average performance of the right only ($n = 11$), left only

Table 2. Exp. 1: Biological motion perceptual thresholds of patients and controls

Patient	Threshold	Versus brain-damaged controls (control group 3)													
		Versus healthy age-matched controls (control group 1)				All (<i>n</i> = 54)		LH damage only (<i>n</i> = 43)		RH damage only (<i>n</i> = 11)		With "critical" pSTS lesion (<i>n</i> = 9)		With "critical" vPMC lesion (<i>n</i> = 10)	
		Mean threshold ± SD	<i>t</i>	<i>P</i>	<i>t</i>	<i>P</i>	<i>t</i>	<i>P</i>	<i>t</i>	<i>P</i>	<i>t</i>	<i>P</i>	<i>t</i>	<i>P</i>	
EL	18.38	19.15 ± 8.74	-0.086	0.933	1.47	0.15*	1.5	0.14*	1.29	0.22*	4.187	0.002*	3.66	0.003*	
GB	18.73	19.15 ± 8.74	-0.047	0.963	1.54	0.13*	1.57	0.12*	1.35	0.20*	4.319	0.002*	3.78	0.003*	
SH	11.33	19.15 ± 8.74	-0.866	0.401	0.12	0.90	0.09	0.93	0.22	0.83	1.528	0.082*	1.27	0.117*	
CR	13.97	28.66 ± 7.91	-1.8	0.09	0.63	0.53	0.62	0.53	0.62	0.54	2.52	0.018*	2.17	0.03*	
SM	12.25	25.06 ± 7.54	-1.64	0.12	0.3	0.77	0.27	0.78	0.36	0.72	1.875	0.049*	1.58	0.07*	
EC	9.57	20.08 ± 7.87	-1.29	0.22	-0.21	0.83	-0.26	0.79	-0.047	0.96	0.864	0.206*	0.676	0.26*	

Thresholds indicate the number of noise points masking the stimuli while performance is at 82% accuracy (Methods). Statistical values (*t*, *P*) represent single-case vs. control group comparisons (40). Ventral visual patients' perceptual thresholds for biological motion were not significantly different from those of three control groups: healthy age-matched (group 1), brain-damaged (group 3), and younger controls (group 2; see Results). Importantly, the group of ventral patients performed significantly better than the group of patients with lesions to pSTS or vPMC (Results).

*At the upper end of the controls' distribution (i.e., performing better than the average).

(*n* = 43), or combined right and left hemisphere brain-damaged control patients (see Table 2 for full details). All of these comparisons indicate that the six ventral patients performed well within the range of other (nonventral) brain-damaged patients, thereby ruling out a specific role for the ventral cortex in biological motion perception.

The data from the control brain-damaged patients were taken from a previous study (11) that revealed that lesions to the left pSTS (L-pSTS) or to left vPMC (L-vPMC) had the greatest adverse effect on biological motion perception. The function and structure of these regions are associated with biological motion perception (11, 15, 16, 20, 41–45) and their role in biological motion perception has been confirmed in several TMS studies (15, 16). In light of this finding, these data permit a stringent comparison between the performance of our ventral patients and that of the brain-damaged patients with lesions to L-pSTS or L-vPMC (the two "critical" lesion groups). As shown in Fig. 1C, the ventral visual patient group performed significantly better (had higher perceptual thresholds, meaning they could tolerate more noise points) than both of the critical lesion groups [Wilcoxon nonparametric rank-sum test: ventral patients (median = 13.11, *n* = 6) vs. lesioned L-pSTS (median = 7.1, *n* = 9): *U* = 73, *P* = 0.0016; ventral patients vs. lesioned L-vPMC (median = 7.6, *n* = 10): *U* = 77, *P* = 0.003]. Furthermore, in single-case comparisons [each ventral patient vs. the critical control groups (40)], four of the ventral visual patients performed significantly better than the critical control groups (Table 2). These results indicate that damage to the ventral visual cortex, unlike damage to the pSTS or vPMC, does not impair biological motion perception.

Response times for biological motion. The results thus far indicate that biological motion perception does not rely on ventral stream integrity. To confirm this finding and ensure that the results were not a product of a speed-accuracy trade-off, we examined reaction times even though participants were informed that speeded responses were not required and participants were allowed to speak and take breaks during the experiment (Fig. 1D). The responses of the patients were not significantly slower than their age-matched controls [Wilcoxon nonparametric rank-sum test: ventral patients (median = 7.78 s, *n* = 6) vs. age-matched controls (median = 5.21 s, *n* = 33): *U* = 159, *P* = 0.134, *z* = 1.5]. This finding also held true for five ventral patients under single-case comparisons of patient vs. age-matched control group [two-tailed, *|t|*s < 0.5, *Ps* > 0.63 (40)]. EC was significantly slower than her age-matched controls [*t*₍₁₁₎ = 4.74, *P* = 0.0008]; however, this is almost certainly a result of the fact that she spoke during the experiment. These results confirm that reaction times were within the normal

range for the ventral patients and that these normal perceptual thresholds did not result from elongated response times.

Experiment 2. Recognition and perceptual thresholds for biological motion under a different paradigm. To provide additional support for the findings from Exp. 1, we further examined the perceptual thresholds of the ventral patients using a modified biological motion experimental paradigm. This task included a larger set of biological motion animations, different presentation and task requirements, and provided feedback. In this experiment, each trial consisted of one centrally displayed PLD (Fig. 2A) and observers determined whether there was a moving human figure embedded in the display (compare Fig. 2A, Center and Right; see Methods). During the action-recognition phase (Fig. 2A, Left), all ventral patients and their controls effortlessly reported the actions present in the PLDs. Moreover, the ventral patients' perceptual thresholds fell within the normal range of their age-matched controls (Fig. 2B and Table S1) [CR: *t*₍₁₄₎ = -1.42, *P* > 0.17; SM: *t*₍₁₄₎ = -0.88, *P* > 0.39; EC: *t*₍₁₄₎ = -0.76, *P* > 0.45; EL: *t*₍₁₀₎ = 0.30, *P* > 0.77; GB: *t*₍₁₀₎ = 1.56, *P* > 0.15; SH: *t*₍₁₀₎ = -0.65, *P* > 0.53]; the performance of EL, GB, and SH also fell in the normal range of a bigger control group (*n* = 14), aged 60.2 ± 6.45 (SD): *|t*₍₁₃₎s < 0.5, *Ps* > 0.6.] Of great interest, the perceptual thresholds established here for each of the patients (and the relative rank ordering of the patients) were very similar to those obtained in Exp. 1, reflecting the reliability and consistency of these measures.

Response times for biological motion under a different paradigm. The analysis of the reaction times of the patients versus the age-matched controls revealed no significant group differences (Fig. 2C) [all patients but EL: *|t|*s < 0.79, *Ps* > 0.45, EL: *t*₍₁₀₎ = 1.51, *P* > 0.16], again confirming that the patients performed within the normal range.

Subjective Reports About Biological Motion Perception. As a converging source of evidence, we obtained self-reports from the patients and controls in response to questions such as whether, on the basis of gait, they were able to recognize individuals and discriminate the age and sex of an individual and, for the patients, whether these abilities have changed postinjury. All patients, as well as controls, reported that they were able to comprehend movement patterns and actions even when they were unable to recognize the person doing it. Subjects also reported that they were able to discriminate sex and age based on gait, and that they could easily recognize atypical gait (e.g., limping). None of the patients reported that their abilities changed following their brain injury. Although these reports are

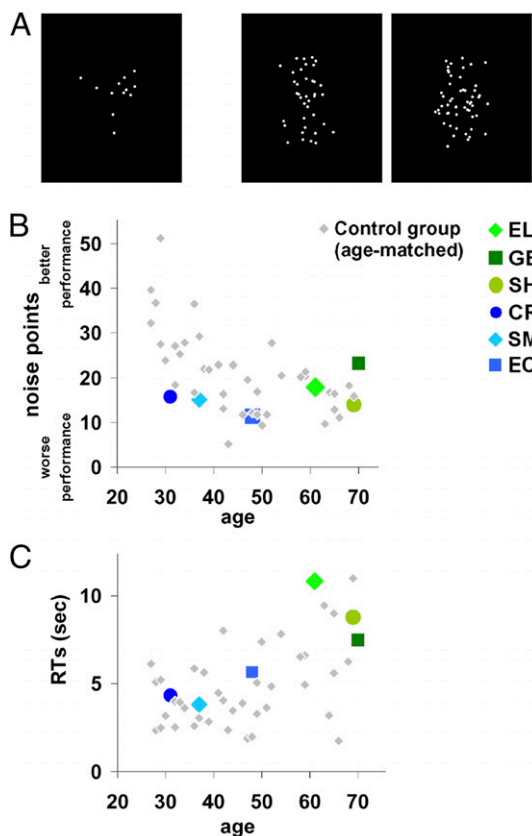


Fig. 2. Biological motion perception: Exp. 2 paradigm and results. (A, Left) Static unmasked PLD snapshot presented in the action recognition phase, participants were required to verbally describe them. (Center and Right) To determine perceptual thresholds, each trial presented a masked PLD either containing a biologically moving figure (Center) or a spatially scrambled version of it (Right), and the task was to determine whether a moving figure was embedded in the display. The noise points were added adaptively according to individual performance with 75% accuracy (Methods). (B) Individual perceptual thresholds (y axis) of the ventral visual patients and the age-matched controls against age (x axis). Perceptual thresholds determined similar to Fig. 1 (Methods). Although patients commonly perform more poorly than healthy-matched controls, the performance of each ventral patient was not significantly different from that of their healthy age-matched controls (Results). (C) Response times are not very informative because instructions did not require speeded responses (participants were able to respond leisurely and take breaks). Ventral visual patients' response times were not significantly slower than their age-matched controls (Results).

subjective, they provide additional indications that biological motion perception may be dissociable from form perception.

Relationship of Perceptual Performance to Underlying Lesion. The experimental findings reveal that the six ventral patients performed as well as or even better than (see comparison against patients with frank pSTS or vPMC lesions) the various control groups. We have proposed that the dissociation between the deficit in form perception and their intact biological motion perception rules out the functional contribution of the ventral cortex.

A possible alternative explanation, however, is that because the ventral cortex is so extensive and lesions are more circumscribed, there may be sparing of key ventral regions associated with biological motion processing (13), and it is these spared regions that account for the normal perceptual performance. To assess this possibility, we first carefully delineated the lesion of each patient and transformed each lesion into normalized Montreal Neurological Institute (MNI) space. Second, we superimposed the lesion

onto the ventral cortex in which we identified areas that are consistently activated by biological motion; this included regions responsive to the perception of body movement (blue in Fig. 3), sensitive to static bodies (yellow in Fig. 3), to human movements (green in Fig. 3) as determined by a recent meta-analysis (13) (Methods), as well as motion-sensitive MT+/V5, biological motion-sensitive pSTS, vPMC, and static-body sensitive EBA (18–20). For the EBA cluster, we further distinguished between three subregions: the ventral portion (v-EBA, ventral and not overlapping MT+/V5), the portion overlapping MT+/V5 (mt-EBA), and the portion anterior to MT+/V5 (a-EBA). Our analysis also took into consideration the functional anatomical organization of the ventral visual stream (e.g., ventral surface vs. lateral occipito-temporal aspects). Third, for each of these regions, we evaluated the extent of damage in each patient. The results of this fine-grained analysis are detailed in Table 3.

Our analysis revealed that regions situated on the ventral surface (e.g., fusiform gyrus) that are assumed to be engaged in some aspect of biological motion perception, including the regions that are sensitive to static body perception, body movements in general, and human body movements' selectivity (13), are substantially damaged in three patients (60–100%, left regions in GB and SH, and the right regions in EC) (Table 3). Furthermore, the ventral portion of the EBA (46, 47), situated ventrally to but not overlapping MT+/V5, is also critically damaged in two right ventral patients (SM and EC) and partially damaged in the left ventral patient (GB). From these observations, we can conclude that regions situated on the ventral surface of the cortex in the ventral stream (20, 31, 48) and the ventral aspect of the EBA are not contributing critically to biological motion perception. Because other regions, such as those on the lateral occipito-temporal surface, including MT+/V5 and other parts of EBA, are only partially damaged in some of the patients (20–60%), we cannot rule out their possible role in biological motion perception.

Each of the regions associated with biological motion in the ventral aspect of the ventral visual cortex is significantly damaged in one or more of the patients (right fusiform in EC, left fusiform in GB and SH), including the right and left ventral portions of the EBA (R-v-EBA in EC and SM, L-v-EBA in GB), and also left MT+/V5 (EL); the superior and middle temporal regions are mostly spared (except for EL). Importantly, the two areas that are well-known to be sensitive and critical to human motion, the pSTS and vPMC (11, 13, 16, 28, 30, 32, 45, 49), are spared in all cases.

The ventral patients performed as well as healthy controls and brain-damaged patients, despite the fact that ventral regions associated with different aspects of biological motion processing were affected by their lesions. Importantly, the ventral-lesioned patients performed better than patients with brain damage to regions pSTS and vPMC, standardly considered the neural correlates of biological motion perception.

Discussion

In this study, we explored whether the integrity of form perception and of the ventral visual cortex are necessary for the perception of biological motion. This was achieved by examining the perceptual performance of patients with documented form deficits following brain damage to the ventral visual cortex. In two studies using animated PLDs (7) embedded in noise points, we derived a host of dependent measures (accuracy of unmasked displays, thresholds, reaction times, and self-report measures) There were no differences between the patients' indices and those of healthy age-matched controls or of brain-damaged patients* with spared ventral cortex, and this was also true compared with healthy young controls. The

*Biological motion sensitivity following brain damage of any sort can be reduced relative to healthy controls (11), accounting for the findings that some ventral patients performed at the lower end of the healthy control distribution.

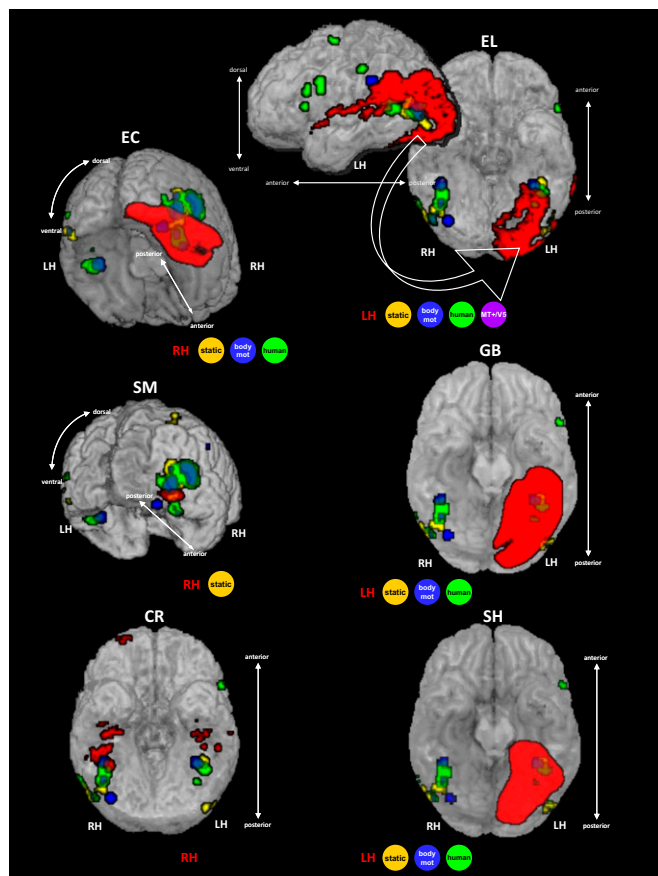


Fig. 3. Situating the patients' lesions with respect to visual regions standardly associated with biological motion processing, presented in rendered fashion. Lesion of each patient is delineated in red based on the structural images (*Methods* and *Supporting Information*). Regions consistently associated with biological motion processing are based on statistical maps of a meta-analysis (13): regions in blue are significantly activated to biological motion, regions in yellow are sensitive to static bodies, and regions in green are sensitive to human movement over nonhuman movements. As summarized in Table 3, ventral visual regions associated with all of the three types of biological motion perception were severely affected by brain damage in one or more of the ventral visual patients, including the ventral aspect of EBA (v-EBA, in EC, SM, and GB). This finding indicates that the spared perceptual thresholds for biological motion perception do not rely on the integrity of the ventral visual regions associated with biological motion processing. MT+/V5, middle temporal motion sensitive region; RH/LH, right/left hemisphere. See also Table 3.

fact that the performance of each of the patients was not significantly different from that of three different control groups, and that this result was replicated across different paradigms, suggests that we are not failing to detect a deficit. Moreover, the patients performed significantly better than patients with documented damage to regions critical for biological motion perception (pSTS and vPMC) (11). Furthermore, by showing that large swaths of cortex—assumed to be associated with biological motion perception—were lesioned in these patients, we were able to determine that the integrity of the ventral aspects of the ventral visual pathway is not critical for normal biological motion perception.

Hemispheric Contribution to Biological Motion Performance? We consider it unlikely that the interindividual variability in the ventral patients' biological motion performance is associated with the anatomical variations in brain damage. First, interindividual variability in biological motion perception is consistently found in healthy and nonhealthy populations (43, 50) (Figs. 1*B* and 2*B*). Interestingly, the severity of face or object perception deficits,

which is influenced by the lesioned hemisphere (left with milder and right with severe deficits) did not correlate with biological motion performance either, because SH, who suffers mild face/object perception deficits, performed similarly to CR and SM, both of whom have severe face and object perception deficits. Second, performance following bilateral ventral damage (e.g., CR) was not worse than that of some patients with unilateral cortical damage (SM, EC, or SH). This result is in line with previous findings that individuals with bilateral damage to (WH) (38) or abnormal function of (LG) (51) the ventral visual cortex can successfully recognize biological motion displays. Third, lesion size was also not indicative of performance because CR, SM, and SH, all of whom have comparable performance (Figs. 1*B* and 2*B*), have very different lesion sizes (Table 3), whereas EL and GB, who have extensive lesions, performed best. On the other hand, spared bilateral ventral visual cortex does not suffice for normal biological motion performance when there is unilateral damage to regions critical to biological motion perception [sustained damage (11) or temporary lesions induced by TMS (16)]. Thus, it seems reasonable to conclude that the behavioral variability among our cohort of patients with ventral damage was a reflection of the variability in the general population, and that performance is not dependent on the specific anatomy of the ventral visual lesion.

The Role of the Ventral Visual Pathway in Biological Motion Processing.

Ventral and occipito-temporal regions, which comprise the ventral visual cortex, are associated with the processing of form information ("form pathway"). Perhaps surprisingly, these very regions, including the EBA, are activated in neuroimaging studies that focus on biological motion (refs. 13, 18, 19, 30; Figs. 3 and 4). A possible explanation for the engagement of these areas in biological motion processing is that form-based computations may be implicated in biological motion processing (7, 21–25). Indeed, some have suggested that PLDs might be better characterized as "motion-from-form" (26), and recent models of biological motion recognition have proposed that biological motion recognition computations can be based on a sequence of static form snapshots derived from the movement itself (52, 53) (Fig. 4*A*). Some support for this comes from physiological recordings in nonhuman primates, where biological motion-sensitive neurons show sensitivity to body form in addition to, or instead of, body motion (54–56).

The key question is whether the engagement of these cortical ventral areas is functionally relevant for the perception of biological motion. The answer cannot be reached based on findings from functional imaging and, thus, determining causality remains elusive. Our results indicate that intact ventral regions in the form visual pathway (e.g., along the fusiform gyrus) are not necessary for biological motion perception. Why are these areas activated then, as revealed in neuroimaging investigations? One possibility is that, following damage to the ventral visual cortex, cortical function is reorganized such that other regions become critical for biological motion perception, as perhaps the lesions may have altered the relative contributions of regions in the network supporting biological motion perception. However, notably, all of our patients performed within the normal range of other brain damaged, and notably, nonbrain-damaged control participants. This result indicates that if any such adaptive plasticity occurs, it is surprisingly effective. An alternative possibility, and the one we favor, is that these ventral regions play a role in the representation of the actor and his or her identity and, hence, are activated during biological motion processing. Specifically, a series of static posture snapshots may suffice for a whole-body viewpoint-based representation of the actor (Fig. 4*A*). Thus, whereas actor recognition and the form executing the motion may be computed by the ventral form pathway, the motion kinematics themselves may be computed by the motion pathway (Fig. 4*A*). When the ventral aspects of the ventral visual

Table 3. Summary of patients' lesions

Affected area		EL	GB	SH	CR	SM	EC
Lesioned hemisphere		Left	Left	Left	Right (+ left)	Right	Right
Lesion extent		Extensive	Extensive	Extensive	Intermediate	Small	Extensive
Lesion approximate size in native* space (mm ³)		43,028	49,929*	31,751*	1,510	952	62,959*
Lesion overlap: ventral surface	Regions sensitive to human movements	No	Mostly	All	No	Hardly	Mostly
	Regions sensitive to static bodies	No	All	All	No	Partially	All
	Regions activated to body movement	No	All	All	No	Hardly	Mostly
Lesion overlap: lateral occipito-temporal surface	Regions sensitive to human movements	Partially	Hardly	No	No	No	Mildly
	Regions sensitive to static bodies	Partially	No	No	No	No	Mildly
	regions activated to body movement	Partially	No	No	No	No	Hardly
	MT+/V5	Partially	No	No	No	No	Partially (?)
EBA partitions	v-EBA	No	Partially	No	No	Mostly	All
	mt-EBA	Partially	Hardly	No	No	No	Hardly
	a-EBA	Mildly	No	No	No	No	Partially
Other	pSTS	Mildly	No	No	No	No	No
	vPMC	No	No	No	No	No	No
	Parietal	No	No	No	No	No	No

The lesion size is based on the results of the lesion delineating procedure (see also *Supporting Information*). Because of the low spatial coverage of GB's, SH's, and EC's clinical scans, their lesion size reflects a spatial interpolation across the lesion locations in the clinical images that were available. The assessment of the overlap of the lesion with regions associated with biological motion processing is predominantly based on a recent meta-analysis (13) (see text for details), as demonstrated in Fig. 3. Overlap with MT+/V5 is based on SM's functional localization, and on MT+/V5 reported location for the other patients (81) (*Methods*). Overlap scale relates to foci reported in the meta-analysis with $z \geq 3.2$ score (equivalent to $P \leq 0.0005$). Overlap notations: No, none; Hardly, $<10\%$; Mildly, $\sim 10\text{--}20\%$; Partially, $\sim 20\text{--}60\%$; Mostly, $>60\text{--}70\%$; All, 100%. Regions that are significantly damaged are indicated in bold and shaded gray according to the extent of damage (Mostly to All in dark gray, Partially in medium gray, and Mildly in light gray). EBA partitions: v-EBA, aspect of EBA ventral to MT/V5; mt-EBA, aspect of EBA overlapping MT/V5; a-EBA, aspect of EBA anterior to MT/V5 (46, 47).

*GB's, CR's, and EC's lesion sizes were approximated on an MNI template brain and therefore provided in MNI normalized space units (mm³), which might be an overestimation relative to native space volume (82).

cortex are damaged (an example is conveyed in Fig. 4A by red-colored markings based on our ventral visual patients), snapshots leading to actor recognition might be disrupted. However, because the computations of kinematics mediated by the motion pathway are not significantly affected, movement perception is unaffected. Fig. 4B shows the prediction of this model for PLDs to illustrate our current findings. In addition to the supporting evidence from our patients, as well as from studies of individuals with developmental agnosia (51, 57), form-based and motion-based processing of body motion can be dissociated among healthy controls (50).

Parallel Processing Routes Supporting Biological Motion Perception?

The notion that biological motion perception might be computed in more than one way is also compatible with findings from a series of neuropsychological case studies. For example, LM, the "motion blind" patient with lesioned bilateral MT+/V5 (36), and AF, with severe damage to the dorsal cortex (35), are both able to recognize unmasked PLDs above chance. In addition, patients with brain damage or abnormal vision, such as patient MM (37), who recovered from long-term visual deprivation, or patient JW, who has widespread occipital damage following hypoxia (58), are both able to successfully recognize unmasked PLDs. Finally, the above-chance biological motion performance of patients with lesions that appear to invade early visual areas (35, 59) and are very different from the lesions of the patients examined in the present study, also seems to suggest multiple processing routes supporting biological motion perception.

Although all of these findings are consistent with an account in which biological motion perception may be achieved via multiple pathways, there is still some selectivity to the processing, and there are indications that biological motion perception is independent from other lower-level motion perception. For example, performance in biological motion and motion-coherence tasks are not correlated, as revealed in studies of patients (11), following congenital cataracts (60), or in healthy controls (43). Indeed, all of our ventral patients performed normally in the biological motion tasks but some have basic motion perception deficits [SM, CR, and EC are impaired in motion coherence and motion detection tasks (61)]. Similarly, patients AF and LM performed poorly on early motion tasks despite above-chance performance on biological motion (35, 36).

If biological motion recognition can be achieved via multiple pathways, this duplication might reflect the importance of this process to a multiplicity of abilities, such as social communication, motor learning, and theory of mind. Whether these pathways achieve movement recognition independently remains to be resolved. What is certain, though, is that the integrity of the ventral aspects of the ventral visual stream is not, in and of itself, critical for the normal perception of biological motion.

Conclusions

We have shown that biological motion perception can be achieved despite damage to the ventral aspect of the form visual pathway (e.g., fusiform body area, v-EBA). Although regions such as the

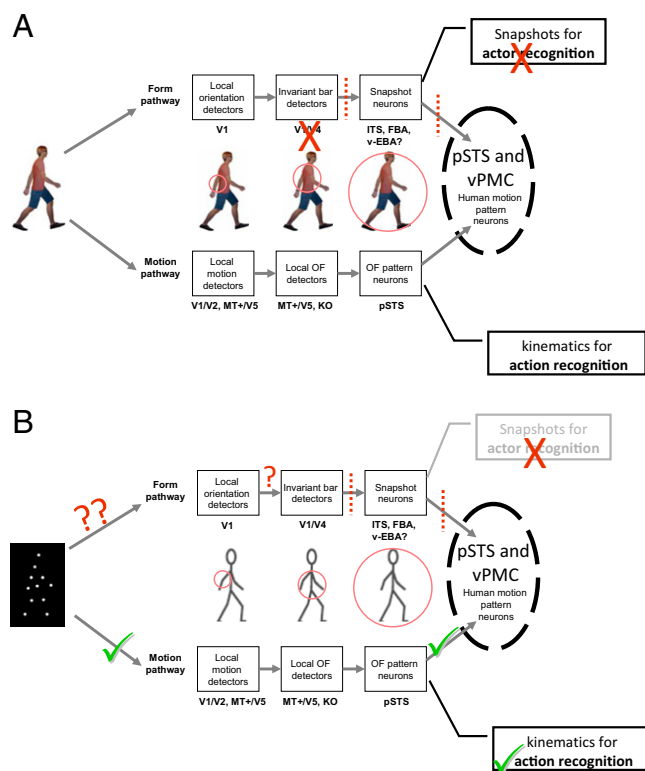


Fig. 4. Adaptation of the model for biological motion recognition based on Giese and Poggio (52). (A) The original model by Giese and Poggio with proposed distinctions: the form pathway's main role involves snapshots for actor recognition, and the motion pathway's main role involves kinematic patterns for human movement recognition. Brick color indicates how brain damage to the ventral cortex predominantly affects the form processing pathway that is involved in snapshot creation, thereby impairing actor but not action recognition. (B) Adaptation of the model to PLDs. Information flow in the case of PLDs resembles that of a damaged ventral visual cortex (A), because the information processed by the form pathway is insufficient, leading to abnormal actor recognition. At the same time, the information processed by the motion pathway is not significantly affected, so that the movement can be recognized. Based on our results, we speculate that the perception of human movement can be achieved based on motion kinematics alone. FBA, fusiform body area; ITS, inferior temporal sulcus; KO, kinetic occipital; MT+/V5, middle temporal motion-sensitive region; OF, optic flow; V1/V2/V4, visual retinotopic regions; v-EBA, ventral aspect of extrastriate body area.

pSTS and vPMC are critical for biological motion perception (11, 15, 16, 41, 62, 63), we speculate that the ventral regions of the form visual pathway are critical for recognizing the person performing the movement, but not for recognizing the motion being performed.

Methods

Patients with Ventral Visual Lesions. Six pre-morbidly normal right-handed individuals who sustained brain damage to the right ($n = 2$), left ($n = 3$), or bilateral ($n = 1$) ventral visual cortex participated in the study. Following a lesion sustained in adulthood (except for CR, who was aged 16 y), all individuals reported visual perceptual problems and have well-established form-processing deficits. Table 1 summarizes the key demographics, neuropsychological descriptions, and detailed visual performance (including visual motion perception) of each patient; further details are available in *Supporting Information* and in earlier publications [SM (61, 64–70), CR (61, 65–67, 70), EL (61, 70–75), GB (61, 75), SH (70, 75), and EC (61)].

Experiment 1. In this experiment, we used unmasked PLDs to assess recognition of biological motion and then measured perceptual thresholds using PLDs masked in noise points. To assess recognition of biological motion, unmasked PLD animations of actions (see below) were presented and participants were required to verbally describe the stimuli without having prior

knowledge of what these would be. Each PLD animation looped until a coherent verbal description was given, after which the experimenter presented the next animation. To measure perceptual thresholds, on each trial two PLDs were presented simultaneously on the right and left sides of the screen, one containing a moving upright human figure performing one of seven actions (see *Stimuli* below) (Fig. 1A, *Supporting Information*, and *Movies S1–S3*) (11, 51, 76), and the other a spatially scrambled version of the same action. The side of the biological motion animation was randomly determined on each trial. Participants were instructed to identify which of the two displays contained the animation of the human movement [but did not have to identify the movement (i.e., jogging or walking), except in the action recognition phase; see below]. Both animations (intact and scrambled movements) were embedded in a number of noise points adaptively determined according to the participant's performance (77). The task became more difficult as the number of noise points increased. Perceptual thresholds were determined based on the number of noise points with which a participant could perform at a predefined level of accuracy (82%). Stimuli and further procedures are fully described in *Supporting Information* and elsewhere (11, 51).

Participants. All six ventral-lesion patients, tested in Pittsburgh, PA, and all healthy control participants (tested in Pittsburgh or in London) gave written informed consent to participate in the study and the experiments were approved by local ethics committees (Institutional Review Board, Carnegie Mellon University and University College London). All patients (except SM, who was tested at Carnegie Mellon University) and the older controls were tested at home for maximal convenience.

Procedures regarding the data collection from the nonventral brain-damaged patient control group (control group 3, see below) are provided elsewhere (11). Informed consent was obtained from these patients at the time of testing in accordance with guidelines of the University of California, San Diego and VA Northern California Health Care System Human Research Protections Programs. The findings from these patients have been published previously (11) and we simply adopted the de-identified data to serve as an additional benchmark against which to compare the ventral patients' performance.

Healthy controls. All healthy control participants had normal or corrected-to-normal vision, no history of neurological disorders, and were right-handed.

Control group 1 was the first neurologically normal control group that participated in this study and included 42 healthy adults, age-matched to the patients: 16 male control participants served as age-matched controls for CR (mean age $32.0 \text{ y} \pm 2.9 \text{ SD}$); 15 males served as age-matched controls for SM (mean age $35.2 \text{ y} \pm 3.3 \text{ SD}$, 11 of whom were also matched for CR); 13 females and 1 male (matched for SM as well) served as age-matched controls for EC (mean age $48.0 \text{ y} \pm 3.8 \text{ SD}$); and 14 females and 1 male served as age-matched controls for GB, EL, and SH (aged 50–70 y, mean $59.2 \pm 6.1 \text{ SD}$, of whom 5 females were matched for EC as well).

Control group 2 was the second neurologically normal control group and included 13 healthy young controls (aged $20.4 \text{ y} \pm 1.1 \text{ SD}$).

Brain-damaged controls. Control group 3 included 54 right-handed, brain-damaged patients (13 females, 41 males, aged 36.9–84.9 y) with focal, unilateral lesions (43 in the left hemisphere, 11 in the right hemisphere). From the 60 patients who had completed Exp. 1 in an earlier study (11), we selected for this control group only those for whom we could definitively determine that their ventral visual cortex was not affected by their lesion (as ascertained and confirmed by the lesion boundaries) as determined from computerized lesion reconstructions of the brain. The time between testing and patients' cerebrovascular accident ranged from 6 mo to 22 y (mean of 6.5 y). Patients with diagnosed or suspected vision or hearing loss, dementia, head trauma, tumors, multiple infarcts, or prior psychiatric or neurological abnormalities were excluded from the sample. Motor and language impairments ranged from very mild to severe in the sample, but all patients were able to understand and carry out the task. None of the patients presented with spatial neglect or other attentional disorders.

Stimuli. Briefly, biological motion PLD animations made of 12 white points on a black background depicting one of seven actions—walking, jogging, overarm throwing, underarm throwing (bowling), stepping up, high kicking into the air, and lower kicking—and lasting 0.8 s were presented and looped until a response was given.

For the perceptual threshold assessment, a matched spatially scrambled version was created for each animation so that the local motion of each point was preserved, without the global form (11, 51, 76).

In each trial of the perceptual threshold assessment, additional moving noise points were randomly superimposed on both PLDs (the biological motion and its scrambled counterpart) (9). The motion trajectory of each noise point that was added to the animations was equivalent to a motion

trajectory of one of the animation's points (randomly chosen), but starting at a random location.

Each animation subtended $\sim 4^\circ \times 6^\circ$ (width \times height) visual angle when viewed from 55 cm. The total area occupied by each PLD (comprising the animation plus the noise points) was $\sim 7^\circ$ of visual angle in diameter. The two PLDs (biological motion and its scrambled counterpart) were displayed at $\sim 9^\circ$ to the left and right of the center of the screen, their vertical centers horizontally aligned (Movie S1). Stimuli were presented and responses recorded using MATLAB (Mathworks) and the Psychophysics Toolbox v2.54 (78, 79).

Procedure. In the first part of the experiment, we examined action recognition of unmasked PLDs. Participants were presented with seven different unmasked biological motion animations and were asked to verbally describe the stimuli on the screen. Each animation was displayed separately in the center of the screen without any masking noise points and looped until the verbal description given by the participant indicated that they were able to perceive the movement conveyed by the PLD animation. After that, the experimenter displayed the next animation.

Following the action-recognition phase, sensitivity to biological motion was assessed by measuring the number of noise dots that allowed successful discrimination (82%) of intact from scrambled animations when both are masked in noise points. On each trial, participants were required to report whether the intact PLD ("the person") was on the right or left side of the screen by pressing the corresponding left or right key in a two-alternative forced-choice (2AFC) manner (see additional details below). The animations looped until a response was given. Although accuracy was the key dependent measure, response time of each trial was also recorded. EC, EL, the brain-damaged controls, and some of the older healthy controls, replied verbally or by pointing, after which the experimenter pressed the corresponding response button. Because the PLDs were presented on the two sides of the screen simultaneously, participants were not required to fixate at the center of the screen. After 16 practice trials with a predefined number of noise points, control participants completed 118 trials presented in two blocks separated by an optional rest period, whereas patients completed one block of 73 trials, with a rest period after 40 trials. Note that because the task was not timed, participants were able to take additional breaks at any time if needed.

To estimate perceptual thresholds, we varied the number of noise points in each trial to yield a psychometric measure of performance according to an efficient Bayesian adaptive procedure that uses the mean of the posterior probability density function [QUEST (77)]. The perceptual threshold was determined as the number of points at which a participant performed at 82% accuracy. For the healthy controls, who performed two blocks of trials, thresholds from the two blocks were averaged. Reaction time analysis was based on each participant's average reaction time across the experiment.

In addition to between-group comparisons, which were based on Wilcoxon nonparametric rank-sum test (80), we also examined every patient's performance individually. This was achieved by determining whether a patient's performance (threshold or reaction time) was significantly different from that of a control group. The statistical evaluation was based on an established statistical procedure for comparing single cases to a control group (40), entailing a modified *t* test, significant performance differences roughly corresponding to more than two SDs from the controls' mean performance.

Experiment 2. The previous experiment assessed the participant's ability to detect the PLD containing human movement when embedded in noise. This second experiment further examined the patients' biological motion perception using a slightly different method, including a different and larger set of displays and a different criterion at which threshold is established.

Participants. All six ventral-damaged patients, tested in Pittsburgh, PA, and 39 healthy neurologically normal controls (28 also participated in Exp. 1) gave informed consent to participate in the study and the experiment was approved by local ethics committees of Carnegie Mellon University (Institutional Review Board) and University College London. The controls were age-matched to each patient in the following way: 15 participants (14 male) served as age-matched controls for CR (mean age 32.5 ± 4.1 SD); 15 participants (12 male) served as age-matched controls for SM (mean age 37.3 ± 4.5 SD, 10 of whom were also matched for CR); 15 participants (12 female) served as age-matched controls for EC [mean age 46.5 ± 4.5 SD, 5/1 controls also matched for SM/CR, respectively]; and 11 participants (8 females) served as age-matched controls for GB, EL, and SH (mean 62.7 ± 4.6 SD, 1 also matched for EC). All patients (but SM, who was tested at Carnegie Mellon University) and some of the controls were tested at home for maximal convenience.

Procedure. We first assessed action recognition of 12 different PLDs (Supporting Information). Participants were asked to describe what they perceived so as to ensure that they were able to recognize the movements conveyed by PLDs. Thereafter, perceptual thresholds were established. A

short practice comprising a few trials with a predefined number of noise points was completed, followed by the main experiment that measured the number of noise points a participant can tolerate and perform at 75% accuracy, using the same Bayesian estimation method as in Exp. 1 (77). In each trial, a single PLD (similar to those from Exp. 1) (Fig. 2A and Supporting Information) was presented at the center of the screen, either containing a movement of an upright human figure performing a movement (target), or a spatially scrambled version of it (nontarget). Animations (targets and nontargets) were masked in noise points (in the same manner as in Exp. 1), and the participant's task was to decide whether the display contained a person ("target present") or not ("target absent") in a 2AFC manner using two predefined keys. Animations looped until a response was given. Visual feedback (green/red cross for correct/incorrect response, respectively) was provided after each response. As in Exp. 1, speeded responses were not required but we still recorded response times. Further experimental details are similar to those of Exp. 1; see details in Supporting Information.

Lesion and Anatomical Analysis. Lesion delineation procedure. For structural image-acquisition details, see Supporting Information. We followed a lesion delineation procedure that has been successfully used before (61). High-resolution anatomical images (EL, SM, and CR) were coregistered onto a T1 MNI canonical SPM image using SPM (www.fil.ion.ucl.ac.uk/spm), after which the lesions were traced manually in MRICroN (www.cabiatl.com/mricro/mricro; see Supporting Information for tracing criteria) and saved as a binary image. For each patient, the coregistered anatomical images and the demarcated lesion were normalized into MNI space using the unified normalization segmentation of SPM. When only low-resolution anatomical images from clinical scans were available, lesions were traced manually onto the corresponding anatomical locations in an MNI canonical SPM image; to provide a consistent visualization of these patients' lesions (Fig. 3), and to reach some approximate assessment of their lesion size (presented in Table 3), their noncontinuous traced lesions were then each manually interpolated to a continuous lesion in a conservative manner using MRICroN (Fig. S1 and Supporting Information).

Comparing lesions to regions associated with biological motion processing. To examine the lesion-behavior relationships, we sited each of our patients' lesions relative to the anatomical locations of regions that are consistently activated across studies in response to biological motion stimuli, as determined by a recent meta-analysis (13). Specifically, we were interested in regions that are consistently activated in response to: (i) body movements [as reported in figure 1 and table 4 of Grosbras et al. (13)], (ii) static bodies [as reported in that study in figure 3 and table 7 of Grosbras et al. (13)], or (iii) human movements vs. nonhuman movements (as reported in table 8 of Grosbras et al. (13)). Three image maps from that meta-analysis corresponding to these three contrasts-of-interest were included in our analysis. Each image map consisted of probability (*P*) values that corresponded to the activation likelihood estimation values reported in Grosbras et al. (13). These maps represent for each specific voxel the probability that a study will report significant activation in that voxel (for example with respect to one of our contrasts-of-interest: regions in which significant activation to human movements vs. nonhuman movements). The maps [as described in Grosbras et al. (13)] were thresholded at $z = 3.2$ (corresponding to $P < 0.0005$) and cluster size was 120 mm^3 [see more details in Grosbras et al. (13)].

For each ventral patient, the three contrasts-of-interest from the meta-analysis along with the normalized brain and delineated lesion were loaded onto MRICroN in four different colors as presented in Fig. 3 [lesion in red, body-movement regions (contrast 1) in blue, static-bodies regions (contrast 2) in yellow, and selective human movements (contrast 3) in green]. We then carefully examined whether the lesion invaded or overlapped any of the regions from each of the three contrasts-of-interest, according to anatomical location as well (e.g., ventral surface vs. lateral occipito-temporal regions). See also Table 3.

ACKNOWLEDGMENTS. We thank all the patients and their families for their wonderful collaboration; Nina Dronkers and the VA Northern California Health Care System; Marie-Helene Grosbras for providing us the image maps from her study (13); and Christina Konen, Solmaz Shariat Torbaghan, Sabine Kastner, Tanja Kassuba, Adam Greenberg, Kate Fissell, Maxim Hammer, Mohamed Seghieh, Ryan Egan, and John Pyles for their help. This study was supported by the Royal Society Grant TG102269 (to S.G.-D. and M.B.); Marie-Curie 236021 (to S.G.-D.); National Science Foundation Grant BCS0923763 and National Institute of Mental Health Grant 54246 (to M.B.); National Science Foundation BCS-CAREER-1151805 (to A.P.S.); and the Wellcome Trust (G.R.). The Wellcome Trust Centre for Neuroimaging is supported by core funding from the Wellcome Trust 091593/Z/10/Z.

1. Billino J, Bremmer F, Gegenfurtner KR (2008) Motion processing at low light levels: Differential effects on the perception of specific motion types. *J Vis* 8(3):1–10.
2. Wood JM, et al. (2011) Using biological motion to enhance the conspicuity of roadway workers. *Accid Anal Prev* 43(3):1036–1041.
3. Tyrrell RA, et al. (2009) Seeing pedestrians at night: Visual clutter does not mask biological motion. *Accid Anal Prev* 41(3):506–512.
4. Balk SA, Tyrrell RA, Brooks JO, Carpenter TL (2008) Highlighting human form and motion information enhances the conspicuity of pedestrians at night. *Perception* 37(8):1276–1284.
5. Owens DA, Antonoff RJ, Francis EL (1994) Biological motion and nighttime pedestrian conspicuity. *Hum Factors* 36(4):718–732.
6. Neri P, Morrone MC, Burr DC (1998) Seeing biological motion. *Nature* 395(6705):894–896.
7. Johansson G (1973) Visual perception of biological motion and a model for its analysis. *Percept Psychophys* 14(2):201–211.
8. Pinto J, Shiffrar M (1999) Subconfigurations of the human form in the perception of biological motion displays. *Acta Psychol (Amst)* 102(2-3):293–318.
9. Bertenthal B, Pinto J (1994) Global processing of biological motion. *Psychol Sci* 5(4):221–225.
10. Pavlova M, Staudt M, Sokolov A, Birbaumer N, Krägeloh-Mann I (2003) Perception and production of biological movement in patients with early periventricular brain lesions. *Brain* 126(Pt 3):692–701.
11. Saygin AP (2007) Superior temporal and premotor brain areas necessary for biological motion perception. *Brain* 130(Pt 9):2452–2461.
12. Wood JM, Tyrrell RA, Carberry TP (2005) Limitations in drivers' ability to recognize pedestrians at night. *Hum Factors* 47(3):644–653.
13. Grosbras MH, Beaton S, Eickhoff SB (2012) Brain regions involved in human movement perception: A quantitative voxel-based meta-analysis. *Hum Brain Mapp* 33(2):431–454.
14. Kourtzi Z, Krelberg B, van Wezel RJ (2008) Linking form and motion in the primate brain. *Trends Cogn Sci* 12(6):230–236.
15. Grossman ED, Battelli L, Pascual-Leone A (2005) Repetitive TMS over posterior STS disrupts perception of biological motion. *Vision Res* 45(22):2847–2853.
16. van Kemenade BM, Muggleton N, Walsh V, Saygin AP (2012) Effects of TMS over premotor and superior temporal cortices on biological motion perception. *J Cogn Neurosci* 24(4):896–904.
17. Vaina LM, Gross CG (2004) Perceptual deficits in patients with impaired recognition of biological motion after temporal lobe lesions. *Proc Natl Acad Sci USA* 101(48):16947–16951.
18. Downing PE, Jiang Y, Shuman M, Kanwisher N (2001) A cortical area selective for visual processing of the human body. *Science* 293(5539):2470–2473.
19. Peelen MV, Downing PE (2007) The neural basis of visual body perception. *Nat Rev Neurosci* 8(8):636–648.
20. Jastorff J, Orban GA (2009) Human functional magnetic resonance imaging reveals separation and integration of shape and motion cues in biological motion processing. *J Neurosci* 29(22):7315–7329.
21. Thompson JC, Clarke M, Stewart T, Puce A (2005) Configural processing of biological motion in human superior temporal sulcus. *J Neurosci* 25(39):9059–9066.
22. Beintema JA, Lappe M (2002) Perception of biological motion without local image motion. *Proc Natl Acad Sci USA* 99(8):5661–5663.
23. Lu H (2010) Structural processing in biological motion perception. *J Vis* 10(12):13.
24. Reid R, Brooks A, Blair D, van der Zwan R (2009) Snap! Recognising implicit actions in static point-light displays. *Perception* 38(4):613–616.
25. Thirkettle M, Scott-Samuel NE, Benton CP (2010) Form overshadows 'opponent motion' information in processing of biological motion from point light walker stimuli. *Vision Res* 50(1):118–126.
26. Lange J, Georg K, Lappe M (2006) Visual perception of biological motion by form: A template-matching analysis. *J Vis* 6(8):836–849.
27. Troje NF (2008) Biological motion perception. *The Senses: A Comprehensive Reference, Vol 1*, eds Basbaum A, et al. (Elsevier, Oxford), pp 231–238.
28. Vaina LM, Solomon J, Chowdhury S, Sinha P, Belliveau JW (2001) Functional neuroanatomy of biological motion perception in humans. *Proc Natl Acad Sci USA* 98(20):11656–11661.
29. Beauchamp MS, Lee KE, Haxby JV, Martin A (2002) Parallel visual motion processing streams for manipulable objects and human movements. *Neuron* 34(1):149–159.
30. Grossman ED, Blake R (2002) Brain areas active during visual perception of biological motion. *Neuron* 35(6):1167–1175.
31. Peelen MV, Wiggert AJ, Downing PE (2006) Patterns of fMRI activity dissociate overlapping functional brain areas that respond to biological motion. *Neuron* 49(6):815–822.
32. Pyles JA, Garcia JO, Hoffman DD, Grossman ED (2007) Visual perception and neural correlates of novel 'biological motion'. *Vision Res* 47(21):2786–2797.
33. Grossman ED, Jardine NL, Pyles JA (2011) fMR-adaptation reveals invariant coding of biological motion on human STS. *Front Hum Neurosci* 5:12.
34. Schenk T, Zihl J (1997) Visual motion perception after brain damage: II. Deficits in form-from-motion perception. *Neuropsychologia* 35(9):1299–1310.
35. Vaina LM, Lemay M, Bienfang DC, Choi AY, Nakayama K (1990) Intact "biological motion" and "structure from motion" perception in a patient with impaired motion mechanisms: A case study. *Vis Neurosci* 5(4):353–369.
36. McLeod P, Dittrich W, Driver J, Perrett D, Zihl J (1996) Preserved and impaired detection of structure from motion by a "motion blind" patient. *Vis Cogn* 3(4):363–391.
37. Fine I, et al. (2003) Long-term deprivation affects visual perception and cortex. *Nat Neurosci* 6(9):915–916.
38. Huberle E, Rupek P, Lappe M, Karnath HO (2012) Perception of biological motion in visual agnosia. *Front Behav Neurosci* 6:56.
39. Pavlova M, et al. (2005) Recruitment of periventricular parietal regions in processing cluttered point-light biological motion. *Cereb Cortex* 15(5):594–601.
40. Crawford JR, Howell DC (1998) Comparing an individual's test score against norms derived from small samples. *J Clin Exp Neuropsychol* 12(4):482–486.
41. Saygin AP, Wilson SM, Hagler DJ, Jr, Bates E, Sereno MI (2004) Point-light biological motion perception activates human premotor cortex. *J Neurosci* 24(27):6181–6188.
42. Sereno MI, Saygin AP, Hagler DJ, Jr (2003) Retinotopy in parietal and temporal cortex. *Neuroimage* 19:51523.
43. Gilaie-Dotan S, Kanai R, Bahrami B, Rees G, Saygin AP (2013) Neuroanatomical correlates of biological motion detection. *Neuropsychologia* 51(3):457–463.
44. Grossman E, et al. (2000) Brain areas involved in perception of biological motion. *J Cogn Neurosci* 12(5):711–720.
45. Peuskens H, Vanrie J, Verfaillie K, Orban GA (2005) Specificity of regions processing biological motion. *Eur J Neurosci* 21(10):2864–2875.
46. Weiner KS, Grill-Spector K (2011) Not one extrastriate body area: Using anatomical landmarks, hMT+, and visual field maps to parcellate limb-selective activations in human lateral occipitotemporal cortex. *Neuroimage* 56(4):2183–2199.
47. Ferri S, Kolster H, Jastorff J, Orban GA (2013) The overlap of the EBA and the MT/V5 cluster. *Neuroimage* 66:412–425.
48. Schwarzlose RF, Baker CI, Kanwisher N (2005) Separate face and body selectivity on the fusiform gyrus. *J Neurosci* 25(47):11055–11059.
49. Bonda E, Petrides M, Ostry D, Evans A (1996) Specific involvement of human parietal systems and the amygdala in the perception of biological motion. *J Neurosci* 16(11):3737–3744.
50. Miller LE, Saygin AP (2013) Individual differences in the perception of biological motion: Links to social cognition and motor imagery. *Cognition* 128(2):140–148.
51. Gilaie-Dotan S, Bentin S, Harel M, Rees G, Saygin AP (2011) Normal form from biological motion despite impaired ventral stream function. *Neuropsychologia* 49(5):1033–1043.
52. Giese MA, Poggio T (2003) Neural mechanisms for the recognition of biological movements. *Nat Rev Neurosci* 4(3):179–192.
53. Lange J, Lappe M (2006) A model of biological motion perception from configural form cues. *J Neurosci* 26(11):2894–2906.
54. Vangeneugden J, et al. (2011) Distinct mechanisms for coding of visual actions in macaque temporal cortex. *J Neurosci* 31(2):385–401.
55. Jellema T, Perrett DI (2003) Cells in monkey STS responsive to articulated body motions and consequent static posture: a case of implied motion? *Neuropsychologia* 41(13):1728–1737.
56. Singer JM, Sheinberg DL (2010) Temporal cortex neurons encode articulated actions as slow sequences of integrated poses. *J Neurosci* 30(8):3133–3145.
57. Gilaie-Dotan S, Perry A, Bonneh Y, Malach R, Bentin S (2009) Seeing with profoundly deactivated mid-level visual areas: Non-hierarchical functioning in the human visual cortex. *Cereb Cortex* 19(7):1687–1703.
58. Rosenthal O, Behrmann M (2006) Acquiring long-term representations of visual classes following extensive extrastriate damage. *Neuropsychologia* 44(5):799–815.
59. Huberle E, Rupek P, Lappe M, Karnath HO (2009) Perception of global gestalt by temporal integration in simultanagnosia. *Eur J Neurosci* 29(1):197–204.
60. Hadad BS, Maurer D, Lewis TL (2012) Sparing of sensitivity to biological motion but not of global motion after early visual deprivation. *Dev Sci* 15(4):474–481.
61. Gilaie-Dotan S, et al. (2013) The role of human ventral visual cortex in motion perception. *Brain* 136(Pt 9):2784–2798.
62. Pelphrey KA, et al. (2003) Brain activity evoked by the perception of human walking: Controlling for meaningful coherent motion. *J Neurosci* 23(17):6819–6825.
63. Tai YF, Scherfler C, Brooks DJ, Sawamoto N, Castiello U (2004) The human premotor cortex is 'mirror' only for biological actions. *Curr Biol* 14(2):117–120.
64. Behrmann M, Kimchi R (2003) What does visual agnosia tell us about perceptual organization and its relationship to object perception? *J Exp Psychol Hum Percept Perform* 29(1):19–42.
65. Marotta JJ, Genovese CR, Behrmann M (2001) A functional MRI study of face recognition in patients with prosopagnosia. *Neuroreport* 12(8):1581–1587.
66. Gauthier I, Behrmann M, Tarr MJ (1999) Can face recognition really be dissociated from object recognition? *J Cogn Neurosci* 11(4):349–370.
67. Behrmann M, Williams P (2007) Impairments in part-whole representations of objects in two cases of integrative visual agnosia. *Cogn Neurosci* 24(7):701–730.
68. Nishimura M, Doyle J, Humphreys K, Behrmann M (2010) Probing the face-space of individuals with prosopagnosia. *Neuropsychologia* 48(6):1828–1841.
69. Konen CS, Behrmann M, Nishimura M, Kastner S (2011) The functional neuroanatomy of object agnosia: A case study. *Neuron* 71(1):49–60.
70. Behrmann M, Plaut DC (2014) Bilateral hemispheric processing of words and faces: Evidence from word impairments in prosopagnosia and face impairments in pure alexia. *Cereb Cortex* 24(4):1102–1118.
71. McKeef TJ, Behrmann M (2004) Pure alexia and covert reading: Evidence from Stroop tasks. *Cogn Neurosci* 21(2):443–458.
72. Mycroft RH, Behrmann M, Kay J (2009) Visuo-perceptual deficits in letter-by-letter reading? *Neuropsychologia* 47(7):1733–1744.
73. Montant M, Behrmann M (2001) Phonological activation in pure alexia. *Cogn Neurosci* 18(8):697–727.
74. Behrmann M, Nelson J, Sekuler EB (1998) Visual complexity in letter-by-letter reading: "Pure" alexia is not pure. *Neuropsychologia* 36(11):1115–1132.
75. Habekost T, Petersen A, Behrmann M, Starffelt R (2014) From word superiority to word inferiority: Visual processing of letters and words in pure alexia. *Cogn Neurosci* 31(5-6):413–436.
76. Ahlström V, Blake R, Ahlström U (1997) Perception of biological motion. *Perception* 26(12):1539–1548.
77. Watson AB, Pelli DG (1983) QUEST: A Bayesian adaptive psychometric method. *Percept Psychophys* 33(2):113–120.
78. Brainard DH (1997) The Psychophysics Toolbox. *Spat Vis* 10(4):433–436.
79. Pelli DG (1997) The VideoToolbox software for visual psychophysics: Transforming numbers into movies. *Spat Vis* 10(4):437–442.
80. Wilcoxon F (1945) Individual comparisons by ranking methods. *Biom Bull* 1(6):80–83.
81. Kolster H, Peeters R, Orban GA (2010) The retinotopic organization of the human middle temporal area MT/V5 and its cortical neighbors. *J Neurosci* 30(29):9801–9820.
82. Allen JS, et al. (2008) Effects of spatial transformation on regional brain volume estimates. *Neuroimage* 42(2):535–547.

Supporting Information

Gilaie-Dotan et al. 10.1073/pnas.1414974112

Case Descriptions: Additional Details

Left Hemisphere Lesions.

EL case description. EL suffered a left posterior cerebral artery (PCA) infarct affecting the medial temporal lobe and occipital lobe as revealed by a 3T MRI scan (Fig. 3). EL has participated in many previous studies, which provide detailed description of her abilities and impairments (1–7). Briefly, these earlier studies revealed that she has pure alexia as well as some difficulty in object and face recognition. She worked as a reading specialist before her stroke.

GB case description. GB suffered a PCA stroke. An MRI scan performed 3 y poststroke revealed a lesion affecting two-thirds of the left temporal lobe and the inferior aspect of the left occipital lobe (Fig. 3). She suffers from pure alexia and, as uncovered in previous studies (5–7), she has some mild impairment in object and face recognition, too. GB worked as a graphic artist before her stroke.

SH case description. SH suffered from a lesion affecting left temporo-occipital structures and the left thalamus, compatible with a left PCA infarct (Fig. 3). He suffers from pure alexia and, as uncovered in previous studies (6, 7), he has mild impairments in face and object recognition. SH worked as a lawyer before his stroke.

Right Hemisphere Lesions.

SM case description. SM sustained a closed head injury in a motor vehicle accident at the age of 18 and recovered well after rehabilitation, aside from a persisting visual agnosia and prosopagnosia. Recent neuroimaging (8) revealed a circumscribed lesion in the posterior portion of the right lateral fusiform gyrus. Further details of his medical and neuropsychological history can be found in previous studies (5, 6, 9–12). SM works in a photography studio.

CR case description. CR suffered from a right temporal lobe abscess with a complicated medical course, including a history of Group A toxic shock syndrome, pneumonia, cardiac arrest, candida bacteremia, and metabolic encephalopathy in May 1996, ~15 y before his participation in this study. MR scans reveal a right temporal lobe lesion consistent with acute microabscesses of the right temporal lobe and medial occipital lobe, and there are small lacunae in the left hemisphere as well. CR has participated in several previous studies (5, 6, 9, 10, 13) that highlight his visual perceptual deficits, which include impaired recognition of objects and of faces. CR completed community college and now runs a restaurant.

EC case description. EC was tested 4 y after suffering an infarction. The radiology report states that there is low attenuation at the right temporal lobe and right occipital lobe posteriorly, consistent with a right PCA infarct. She showed difficulties in both face and object recognition on screening tests conducted before these experiments (5).

Additional Experimental Details

Experiment 1: Additional Experimental Details. This experiment has been described in detail elsewhere (14, 15). Biological motion animations were created by videotaping an actor performing various activities, and encoding only the joint positions in digitized videos (16). In the movies, the joints were represented by 12 small white points against a black background (Fig. 1A; for an animated example, see Movies S2 and S3).

Each animation consisted of 20 distinct frames and was displayed for 0.5 s (16.5-ms interframe interval, 60 Hz). The final frame then remained visible for 0.3 s, after which the animation looped from the beginning. Because a joint could become oc-

cluded by other body parts during an action, some points were briefly invisible at times.

For each of the animations, the matched spatially scrambled animation was created by scrambling the starting positions of the 12 points while keeping the motion trajectories of each point unchanged. The starting positions of the scrambled points were chosen randomly within a region so that the total area encompassed by the scrambled animation was similar to that of the original nonscrambled biological animation (Fig. 1A).

Experiment 2: Additional Experimental Details.

Stimuli. This experiment included the seven animations from Exp. 1 and five additional ones (climbing stairs, skipping rope, kicking leftward with right leg, bending down, and pitching). All of the animations were created in the same manner as described in Exp. 1. For each animation, a spatially scrambled matched-version animation was created as described in Exp. 1. As in Exp. 1, a variable number of noise points, each with a motion trajectory as one of the points from the target biological motion animation, were also presented on each trial of the perceptual threshold assessment (in each trial, all of the noise point motion trajectories were from the same animation), and the initial spatial location of the noise points was determined randomly.

The PLD that was presented centrally in each trial subtended $\sim 4^\circ \times 8^\circ$ visual angle when viewed from 55 cm while the region populated by the PLD and the noise points together was $\sim 8^\circ \times 12^\circ$ visual angle. On each trial, the target (or nontarget) PLD was presented at a randomly jittered location within a 2.2° radius from the center of the screen. Stimuli were presented and responses recorded using Matlab (Mathworks) and the Psychophysics Toolbox v2.54 (17, 18).

Procedure. The experiment started with assessing action recognition of unmasked PLD animations. The participants were not informed about what they were about to view and were instructed to describe what they saw. Following this phase, we assessed perceptual thresholds. Each participant completed a practice block that included 16 trials with a range of predetermined number of noise points (ranging from 0 to 40). The practice was followed by the main experimental block, which included 60 trials in which the number of noise points was determined in an adaptive manner, contingent on performance, beginning with 10 noise points. Varying the number of noise points enabled us to measure biological motion-detection thresholds at which each participant performed at 75% accuracy (19), and this was done using the same Bayesian adaptive paradigm as in Exp. 1 (QUEST). The task became more difficult with an increasing number of noise points.

Each trial started with a white fixation cross displayed at the center of the screen for 750 ms, after which the PLDs were presented along with noise points. The animations were repeated continuously until a response was given. After each response, a visual feedback cue appeared for 750 ms (green fixation cross for correct, red for incorrect).

Data analysis. Thresholds were calculated for each patient and for each of the control participants, and data (thresholds and response times) were analyzed as in Exp. 1.

SI Results

Experiment 1: Additional Results. We have now also conducted a set of comparisons of ventral patient group vs. matched control group using the perceptual thresholds measured in Exp. 1. In each comparison (two-tailed *t* test assuming unequal variance), we

randomly picked for each patient one control from his or her control group to serve as the matched control for that test so that the groups were matched in size. We then redid this control sampling 10 times. In 6 of the 10 statistical comparisons, there was no significant difference between the ventral patients group and the age-matched control group (P s = 0.502, 0.107, 0.802, 0.197, 0.116, 0.158); in three of the runs there was a borderline effect ($0.05 < P < 0.1$); and in one run there was a significant effect between the groups ($P < 0.05$).

These results are reassuring in showing that in most cases the ventral patients are indeed within the norm of healthy age-matched controls, even at a group level. Also, because it is typical for a group of (any type of) brain-damaged patients to perform significantly more poorly than a group of age-matched controls (*Results*), that we see borderline effects in some comparisons is perhaps not surprising. In addition, given the small sample size, the variability may not be surprising either.

Experiment 2: Additional Results. We also carried out the same group vs. group statistical comparisons that are described above (the set of 10 comparisons for ventral patient group vs. matched control group) with the perceptual thresholds derived in Exp. 2. In 10 of the 10 comparisons, the performance of the patients' group did not significantly differ from that of the matched control group (P s = 0.327, 0.212, 0.547, 0.132, 0.911, 0.579, 0.153, 0.447, 0.608, 0.212). These results further confirm our finding that the ventral patients perform normally on biological motion perception, as evident in a different paradigm.

Ventral Visual Patients' Structural Image Acquisition

EL. EL's anatomical MR scans were acquired at the Brain Imaging Research Center Pittsburgh on a Siemens Allegra MRI 3T scanner using a head coil, when she was 60 y old, approximately 1 y before her participation in this study and 14 y after her injury. The scan acquired 192 MPRAGE sagittal slices (1-mm thickness, inplane resolution of $1 \times 1 \text{ mm}^2$, matrix = 256×256 , repetition time 1,740 ms, echo time 3.04 ms, inversion time 1,000 ms, flip angle = 8°).

GB. GB's MR clinical structural scans were acquired on a 1.5T GE Genesis Signa MR scanner equipped with a head coil, ~ 3 y before her participation in this study. These included 23 axial T2 images (slice thickness = 5.5 mm, 7 mm gap, image size 512×512 , pixel spacing $0.42968 \times 0.42968 \text{ mm}^2$, echo time = 96.512 ms, no. of averages = 2, flip angle = 90°).

SH. SH's CT clinical structural scans were acquired on a Siemens SOMATOM Sensation 4 CT scanner when he was 63 y old, and ~ 6 y before his participation in this study. These included axial images with slice thickness/overlap of 5.0/2.5 mm.

SM. SM's MRI structural scans were acquired with identical parameters to those of EL's (see above) at the Brain Imaging Research Center Pittsburgh when he was 35 y old. This was 17 y after his injury and ~ 2 y before his participation in this study (for details, see ref. 8).

CR. CR's MRI structural scans were acquired at the Magnetic Resonance Research Center, University of Pittsburgh Medical Center on a 1.5T Signa whole-body scanner (General Electric Medical Systems), ~ 3 y after he had metabolic encephalopathy and ~ 12 y before his participation in this study. This included 124 slices of 1.5-mm thickness with an inplane resolution of $0.9375 \times 0.9375 \text{ mm}^2$, matrix of 256×256 .

EC. EC's CT clinical structural scans were acquired on a GE Medical Systems LightSpeed QX/i CT scanner when she was 40 y old, and ~ 8 y before her participation in this study. These in-

cluded 34 axial images without contrast with slice thickness of 2.5 mm (through the posterior fossa) and 7.5 mm (from the posterior fossa to the vertex), 512×512 image size, and pixel spacing of $0.449219 \times 0.449219 \text{ mm}^2$.

Lesion-Tracing Criteria

We used an established procedure and most of these details are published elsewhere (5). We describe below specific modifications we made to document the lesion of each patient, where necessary.

EL. Because the average intensity values varied across each structural image regardless of the lesion (e.g., between anterior and posterior regions, or right and left hemispheres), the definition of the lesioned tissue was not based solely on absolute intensity values, and relative local differences were considered as well. Instead, the definition of the lesioned tissue also took into account abrupt local changes in intensities between lesioned and adjacent healthy tissue, and continuity of abnormal lesioned tissue. Locally, lesioned tissue always had substantially lower values of intensity than healthy tissue. In most parts of EL's brain and around the lesion, healthy tissue-intensity values ranged from 200 to above 350, whereas lesioned tissue-intensity values ranged from 54 to 170. However, in specific locations the value, 170, was considered healthy tissue (adjacent to value of 117 of a lesioned tissue). We provide lesion size estimates based on local intensity variations and continuity assessment, and also a more conservative estimation based on intensity values < 150 in the predefined lesion zone (Table 3).

SM. SM's structural images also revealed local variations in intensity values; thus, as with EL, we delineated the lesion based on intensity values, continuity of the lesioned tissue, and abrupt changes in local intensity values between the lesion and adjacent healthy tissue. Common values for healthy tissue were above 200 to even above 350; however, locally healthy tissue could have value of 171. Lesioned tissue typically had values ranging from as low as 60 to values around 150; however, locally, values of 160 or 174 could be attributed to lesioned tissue. We provide the lesion size estimate according to the criteria laid out above, along with a conservative estimate for the lesion when lesioned intensities are < 160 .

CR. Because CR's lesion is of a different etiology than that of EL and SM, the lesion delineation criteria were different. CR has a definitive lesion in the right temporal lobe (see above) that is evident and confirmed by an expert neuroradiologist in the past and during the present study. In addition, there are foci of petechial hemorrhage seen along the gray/white junction at multiple areas that appear as a very dark center (intensity values of below 35) bordered by very bright intensity tissue (intensity above 120). Healthy tissue in CR's structural images had intensity values of 55–95. There are, however, some small foci of enhancement in the left hemisphere (perhaps resolved abscesses) and so we adopt a conservative approach here and leave open the possibility of additional left hemisphere insult.

GB, EC, and SH. Lesioned tissue in GB's, EC's, and SH's original clinical structural images were used to guide delineation in a normalized MNI canonical brain. GB's original DICOM images were loaded into MATLAB (Mathworks), where intensity values of lesioned tissue were above 0.5 and healthy tissue intensity values were below 0.4. Because of technical issues with MATLAB reading EC's DICOM images, EC's structural images were loaded into MicroDicom (www.microdicom.com) and then exported to bitmap images. Typically, lesioned tissue intensity values were below 105 and healthy tissue values were above 110. In the lesion delineation process we also took into account (as with the other patients) continuity of the lesioned tissue and

abrupt intensity changes between the lesion and adjacent healthy tissue. After the lesion tracing in the original images detailed above, an approximated corresponding delineation was carried out onto a single subject T1 SPM MNI-normalized template. Following that process, we manually interpolated each lesion

into a continuous lesion in a conservative manner. This process was achieved in MRICroN software (www.mricron.com), where the originally traced lesioned volume (in axial sections) was then filled in manually in the orthogonal section planes (sagittal and coronal) by linear interpolation (Fig. S1).

- McKeeff TJ, Behrmann M (2004) Pure alexia and covert reading: Evidence from Stroop tasks. *Cogn Neuropsychol* 21(2):443–458.
- Mycroft RH, Behrmann M, Kay J (2009) Visuo-perceptual deficits in letter-by-letter reading? *Neuropsychologia* 47(7):1733–1744.
- Montant M, Behrmann M (2001) Phonological activation in pure alexia. *Cogn Neuropsychol* 18(8):697–727.
- Behrmann M, Nelson J, Sekuler EB (1998) Visual complexity in letter-by-letter reading: "Pure" alexia is not pure. *Neuropsychologia* 36(11):1115–1132.
- Gilaie-Dotan S, et al. (2013) The role of human ventral visual cortex in motion perception. *Brain* 136(Pt 9):2784–2798.
- Behrmann M, Plaut DC (2014) Bilateral hemispheric processing of words and faces: Evidence from word impairments in prosopagnosia and face impairments in pure alexia. *Cereb Cortex* 24(4):1102–1118.
- Habekost T, Petersen A, Behrmann M, Starrfelt R (2014) From word superiority to word inferiority: Visual processing of letters and words in pure alexia. *Cogn Neuropsychol* 31(5-6):413–436.
- Konen CS, Behrmann M, Nishimura M, Kastner S (2011) The functional neuroanatomy of object agnosia: A case study. *Neuron* 71(1):49–60.
- Gauthier I, Behrmann M, Tarr MJ (1999) Can face recognition really be dissociated from object recognition? *J Cogn Neurosci* 11(4):349–370.
- Marotta JJ, Genovese CR, Behrmann M (2001) A functional MRI study of face recognition in patients with prosopagnosia. *Neuroreport* 12(8):1581–1587.
- Behrmann M, Kimchi R (2003) What does visual agnosia tell us about perceptual organization and its relationship to object perception? *J Exp Psychol Hum Percept Perform* 29(1):19–42.
- Nishimura M, Scherf S, Behrmann M (2009) Development of object recognition in humans. *F1000 Biol Rep* 1:56.
- Behrmann M, Williams P (2007) Impairments in part-whole representations of objects in two cases of integrative visual agnosia. *Cogn Neuropsychol* 24(7):701–730.
- Gilaie-Dotan S, Bentin S, Harel M, Rees G, Saygin AP (2011) Normal form from biological motion despite impaired ventral stream function. *Neuropsychologia* 49(5):1033–1043.
- Saygin AP (2007) Superior temporal and premotor brain areas necessary for biological motion perception. *Brain* 130(Pt 9):2452–2461.
- Ahlström V, Blake R, Ahlström U (1997) Perception of biological motion. *Perception* 26(12):1539–1548.
- Brainard DH (1997) The Psychophysics Toolbox. *Spat Vis* 10(4):433–436.
- Pelli DG (1997) The VideoToolbox software for visual psychophysics: Transforming numbers into movies. *Spat Vis* 10(4):437–442.
- Watson AB, Pelli DG (1983) QUEST: A Bayesian adaptive psychometric method. *Percept Psychophys* 33(2):113–120.

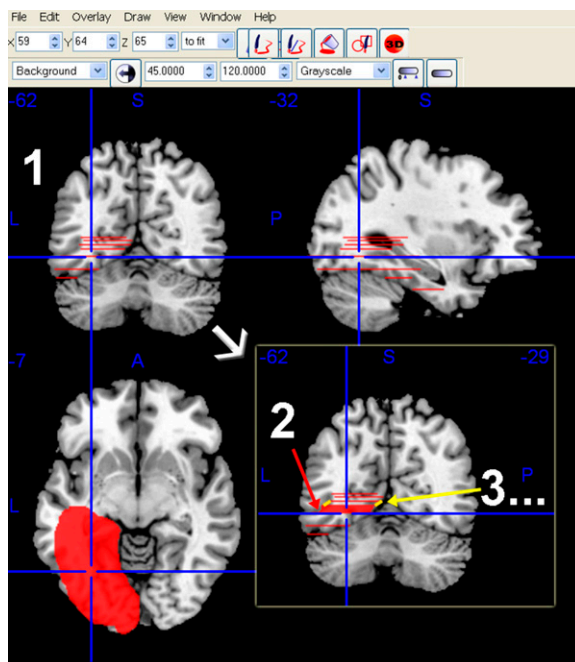
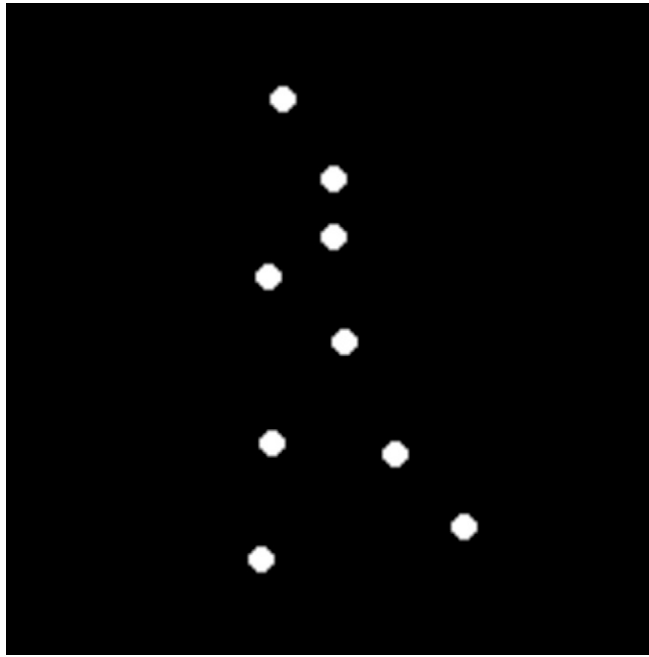


Fig. S1. Demonstration of the filling-in procedure of the traced lesion volume (as was done in the case of GB, EC, and SH). The filling in was achieved by linearly interpolating in the coronal and sagittal planes between the traces of the lesion (in the axial planes, see above *Bottom Left*). One step is shown (in a coronal section) where the interpolation is performed between two traced axial slices (1), and filled in red (2). The step to follow repeats this procedure by filling in the region enclosed by the yellow and red lines (3).



Movie S3. Biological motion animation of a walking upright human figure, which is one of the seven actions used in Exp. 1. This animation was also used in Exp. 2.

[Movie S3](#)